

Surge Phenomena on Power Transmission Line

Daniel Mayer, Bohuř Ulrych

Abstract — The paper presents an algorithm for numerical computation of surge phenomena on a one-phase overhead or cable line with distributed parameters that consists of an arbitrary number of uniform parts. The algorithm was tested on a number of examples, in common with the stability and convergence of solution. The method can be used for calculation of the overvoltage that may occur in the course of feeding transformers or AC rotating machines by voltage containing steep pulses.

I. INTRODUCTION

SOLUTION of the overvoltage phenomena in electrical power networks originating from atmospheric discharges or switching processes is of fundamental importance for design of appropriate protective devices and for assurance of reliable operation of the system. It is also very important for safety of near computer networks and telecommunication devices whose operation can be affected in an undesirable way; overvoltages can lead to considerable material losses caused by damaging of transferred data files or even by destruction of HW.

Many papers deal with theoretical investigation of the overvoltage phenomena only in separate parts of electrical power systems, for example on an overhead or cable line, in the high-voltage winding of a transformer or in the stator winding of an asynchronous or synchronous machine. Distributions of voltages and currents are described by partial differential equations of hyperbolic type in common with the boundary and initial conditions and these equations are solved. But reliable ideas about processes associated with the overvoltage may be obtained only from a complete solution of the whole electrical power system, which leads to much more complicated mathematical models.

The paper represents the first part of the task. It deals with a one-phase line, uniform by parts. Its beginning and end are connected to electric circuits containing lumped parameters R , L and C , that are described by ordinary differential equations. The corresponding mathematical model can be solved analytically, semianalytically or numerically. The analytical solution can be realized, however, in only few specific cases [5]. Some authors (e.g. [2]) applied the Laplace transform, which resulted in a system of ordinary differential and algebraic equations that are much easier to solve. Other authors used semi-analytical approach (originally an analytical way of solution passed at a certain stage to a numerical way (e.g. [1], [4]). Another method is based on an

approximation of the given circuit with distributed parameters by a ladder network consisting of two-ports with lumped parameters, i.e. the circuit is discretized physically. Its analysis can easily be carried out by a suitable professional circuit program. If such a program is unavailable, the mathematical model of the ladder network can be expressed by a system of ordinary differential equations solvable by any good mathematical program. The last way consists in a numerical solution of partial differential equations of the line [3] and this way is dealt with in the paper.

II. CONTINUOUS MATHEMATICAL MODEL

Consider a cascade connection of two uniform lines of lengths d_1 and d_2 . Both lines generally differ by their parameters R_i, L_i, C_i, G_i , $i=1,2$, see Fig. 1. The beginning of line **1** is connected to a source of voltage of a given time evolution and its end to a passive circuit **C** containing lumped parameters R, L, C . Our goal is to find distribution of voltage $u(x,t)$ and current $i(x,t)$ in the definition area $\Omega(x,t)$ where $x \in (0, d_1 + d_2)$, $t > 0$.

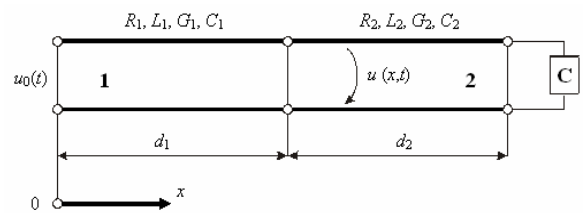


Fig. 1. Arrangement of the investigated one-phase line

Both voltage u and current i in the definition area Ω are described by differential equations (see, for example [5])

$$-\frac{\partial u}{\partial x} = R_n i + L_n \frac{\partial i}{\partial t}, \quad (1)$$

$$-\frac{\partial i}{\partial x} = G_n u + C_n \frac{\partial u}{\partial t}, \quad (2)$$

where $0 < x \leq d_1$ for $n=1$ and $d_1 < x < d_2$ for $n=2$.

The *boundary conditions* read: for $t > 0$

$$x = 0 \Rightarrow F_1(u_0, i_0, t) = 0,$$

$$x = d_1 + d_2 \Rightarrow F_2(u_e, i_e, t) = 0$$

where F_1 and F_2 express relations between voltage and current at the entry **1** and end **2** two-ports of the line, respectively. In a general case, these relations are again systems of ordinary differential equations, in case of simple two-ports we obtain a single differential equation and if the two-port is created by a resistance we have an algebraic equation. If at the entry voltage $u_0(t)$ is applied, we can replace general equation $F_1(u_0, i_0, t) = 0$ by function $u_0(t)$.

The authors are with the Faculty of Electrical Engineering, University of West Bohemia in Pilsen, Sady Pětaticátníků 14, 30614 Plzeň, Czech Republic, E-mail: {mayer, ulrych}@kte.zcu.cz.

This work has been supported by the Research Plan Power and Control Systems of Electromechanical Energy Conversion MSM 232200008.

The *interface conditions* between parts 1 and 2 express continuity of voltage $u(x, t)$ and current $i(x, t)$ for $x = d_1$.

The zero *initial conditions* are accepted for our case: $u(x, 0) = 0$ and $i(x, 0) = 0$.

III. DISCRETE MATHEMATICAL MODEL

Numerical solution of partial differential equations (1) and (2) is carried out by an implicit Wendroff difference approximation (see, for example, [6]). The procedure consists of several steps:

- The system (1) and (2) is first modified in the following way:

$$\frac{\partial u}{\partial x} + k_{11,n}i + k_{12,n} \frac{\partial i}{\partial t} = 0, \quad (3)$$

$$\frac{\partial i}{\partial x} + k_{21,n}u + k_{22,n} \frac{\partial u}{\partial t} = 0 \quad (4)$$

where $k_{11,n} = R_n, k_{12,n} = L_n, k_{21,n} = G_n, k_{22,n} = C_n, n = 1, 2$.

- Continuous definition area Ω of system (3) and (4) is replaced by a uniform spatially-temporal grid of equidistant steps $\Delta x, \Delta t$ so that

- the line of length $d_1 + d_2$ is discretized with a suitable equidistant step Δx , so that we obtain a 1D geometrical grid of $N_1 + N_2$ elements and $N_1 + N_2 + 1$ nodes, where

$$N_1 = d_1 / \Delta x, N_2 = d_2 / \Delta x,$$

- the semibounded temporal coordinate t is discretized with an equidistant step Δt , so that we get a system of discrete time levels $t_l = l \cdot \Delta t$ where $l = 0, 1, 2, \dots$,
- for an arbitrary k -th element of the difference grid we use (according to the scheme shown in Fig. 2) the Wendroff approximation of (3)

$$\begin{aligned} & \frac{1}{2} \left(\frac{u_{k+1,l} - u_{k,l}}{\Delta x} + \frac{u_{k+1,l+1} - u_{k,l+1}}{\Delta x} \right) + \\ & + \frac{k_{11,n}}{4} (i_{k,l} + i_{k+1,l} + i_{k,l+1} + i_{k+1,l+1}) + \\ & + \frac{k_{12,n}}{2} \left(\frac{i_{k,l+1} - i_{k,l}}{\Delta t} + \frac{i_{k+1,l+1} - i_{k+1,l}}{\Delta t} \right) = 0 \end{aligned} \quad (5)$$

and modify it as follows

$$\begin{aligned} & u_{k,l+1} \left(-\frac{1}{2\Delta x} \right) + u_{k+1,l+1} \left(\frac{1}{2\Delta x} \right) + \\ & + i_{k,l+1} \left(\frac{k_{11,n}}{4} + \frac{k_{12,n}}{2\Delta t} \right) + i_{k+1,l+1} \left(\frac{k_{11,n}}{4} + \frac{k_{12,n}}{2\Delta t} \right) = \\ & = u_{k,l} \left(\frac{1}{2\Delta x} \right) + u_{k+1,l} \left(-\frac{1}{2\Delta x} \right) + \\ & + i_{k,l} \left(-\frac{k_{11,n}}{4} + \frac{k_{12,n}}{2\Delta t} \right) + i_{k+1,l} \left(-\frac{k_{11,n}}{4} + \frac{k_{12,n}}{2\Delta t} \right), \end{aligned} \quad (6)$$

- analogously, equation (4) can be (according to the Wendroff difference scheme given in Fig. 3) approximated by expression

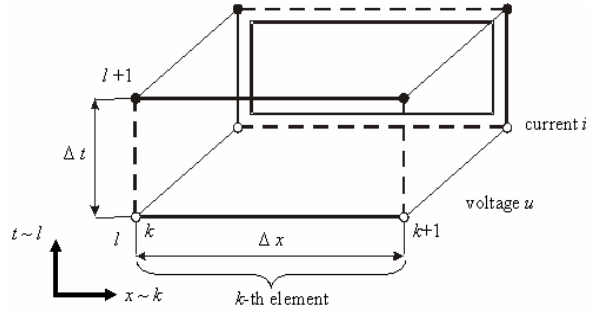


Fig. 2. Scheme of the Wendroff difference approximation of equation (3)

$$\begin{aligned} & \frac{1}{2} \left(\frac{i_{k+1,l} - i_{k,l}}{\Delta x} + \frac{i_{k+1,l+1} - i_{k,l+1}}{\Delta x} \right) + \\ & + \frac{k_{21,n}}{4} (u_{k,l} + u_{k+1,l} + u_{k,l+1} + u_{k+1,l+1}) + \\ & + \frac{k_{22,n}}{2} \left(\frac{u_{k,l+1} - u_{k,l}}{\Delta t} + \frac{u_{k+1,l+1} - u_{k+1,l}}{\Delta t} \right) = 0 \end{aligned} \quad (7)$$

that is rewritten into form

$$\begin{aligned} & u_{k,l+1} \left(\frac{k_{21,n}}{4} + \frac{k_{22,n}}{2\Delta t} \right) + u_{k+1,l+1} \left(\frac{k_{21,n}}{4} + \frac{k_{22,n}}{2\Delta t} \right) + \\ & + i_{k,l+1} \left(-\frac{1}{2\Delta x} \right) + i_{k+1,l+1} \left(\frac{1}{2\Delta x} \right) = \\ & = u_{k,l} \left(-\frac{k_{21,n}}{4} + \frac{k_{22,n}}{2\Delta t} \right) + u_{k+1,l} \left(-\frac{k_{21,n}}{4} + \frac{k_{22,n}}{2\Delta t} \right) + \\ & + i_{k,l} \left(\frac{1}{2\Delta x} \right) + i_{k+1,l} \left(-\frac{1}{2\Delta x} \right). \end{aligned} \quad (8)$$

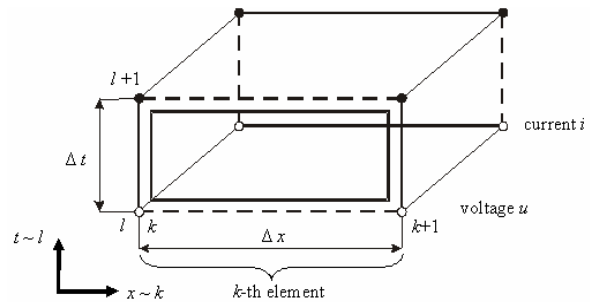


Fig. 3. Scheme of the Wendroff difference approximation of equation (4)

- Modified equations (6) and (8) for all $N_1 + N_2$ elements of the difference grid will create a system of $2(N_1 + N_2)$ equations for $2(N_1 + N_2 + 1)$ unknowns. These equations are supplemented by algebraic approximations of equations $F_1(u_0, i_0, t) = 0$ and $F_2(u_e, i_e, t) = 0$. In case that these equations are algebraic we can include them directly into the system. So we obtain a system of $2(N_1 + N_2 + 1)$ linear algebraic equations that may be written in a matrix description

$$\mathbf{A} \mathbf{X}^{l+1} = \mathbf{B} \mathbf{X}^l, \quad (9)$$

vector \mathbf{X}^{l+1} containing elements $u_{k,l+1}, i_{k,l+1}$ and \mathbf{X}^l elements $u_{k,l}, i_{k,l}, k = 1, \dots, N_1 + N_2 + 1$.

- Solution of (9) provides the values of $u_{k,l+1}, i_{k,l+1}, k = 1, \dots, N_1 + N_2 + 1$ at the $l+1$ -th time level,

starting from values $u_{k,l}, i_{k,l}$, $k = 1, \dots, N_1 + N_2 + 1$ at the previous l -th time level that are known. The algorithm was realized by own code HOMVED 4 written in Borland Delphi.

IV. TESTING EXAMPLE

The algorithm is validated on an example whose analytical solution is known. Beside the verification, we also tested its basic properties, especially its numerical stability and convergence.

A uniform line of length $d = 100$ m ($n = 1$, see chapter 2) and parameters R, L, C, G per unit length fed from a source of harmonic voltage $u_0(t)$ is loaded by resistance R_e . The input data are:

- $u_0(t) = u(0, t) = 100 \sin \omega t$, $\omega = 2\pi f$, $f = 1$ MHz (so that $T_p = 1/f = 10^{-6}$ s),
- $R = 3 \cdot 10^{-3} \Omega/\text{m}$, $L = 3 \cdot 10^{-6}$ H/m, $G = 10^{-9}$ S/m, $C = 8 \cdot 10^{-12}$ F/m,
- $R_e = 1000 \Omega$.

Our task is to find the distribution of voltage $u(x, t)$ along the line in the steady-state operation regime.

The analytical solution to the problem may be expressed (see, for example, [5]) by relation

$$\underline{U}(x) = \underline{U}_0 \left[\cosh \gamma d - \frac{\underline{Z}_0 + \underline{Z}_e \tanh \gamma d}{\underline{Z}_e + \underline{Z}_0 \tanh \gamma d} \sinh \gamma x \right] \quad (10)$$

where

$$\gamma = \sqrt{(R + j\omega L)(G + j\omega C)}, \quad \underline{Z}_0 = \sqrt{\frac{R + j\omega L}{G + j\omega C}} \quad (11)$$

and

$$\underline{U}_0 = 100 + j0, \quad \underline{Z}_e = 1000 + j0.$$

The numerical solution was realized in spatially-temporal area $\Omega(x, t)$ on grids with various steps Δx and Δt satisfying the condition of stability (see, for instance, [4])

$$\Delta t \leq \Delta t_k = \frac{\Delta x}{v} \quad (12)$$

where v denotes the velocity of wave propagation along the line whose value is approximately (see [5])

$$v \approx \frac{1}{\sqrt{LC}}. \quad (13)$$

Integration of equations (1) and (2) was performed for a sufficiently long time in order to reach the steady state. A greater number of numerical computations with various time and space steps were carried out to test the stability and convergence of solution. We started from zero initial conditions and it turned out that the transient took only a relatively short time. The steady state was practically reached for time $t > 5T_p$.

Fig. 4 shows the time evolution of voltage $u_0(t)$ at the beginning of the line (A: $x = 0$) and voltage $u_e(t)$ at its end (C: $x = d$). While damping of the voltage wave is almost negligible, the phase shift between both waveforms A and C is almost 180° . These

results correspond to the analytical solution, $\underline{U}_e = -100.03 - j3.902 \cdot 10^{-2}$ V (see (10, 11), $x = d$).

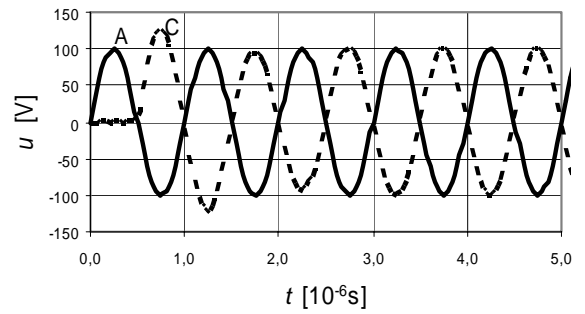


Fig. 4. The testing example: A - voltage $u_0(t)$ at the beginning of the line, C - voltage $u_e(t)$ at the end of the line

Starting from the results obtained, we can draw the following conclusions:

- Solutions that were carried out on a difference grid with steps Δx and Δt satisfying (12) are numerically stable.
- Available accuracy of the numerical solution is fully comparable with the analytical solution.

V. ILLUSTRATIVE EXAMPLE

A cable line of length $d_1 = 50$ m and parameters per unit length $R_1 = 7 \cdot 10^{-4} \Omega/\text{m}$, $L_1 = 4 \cdot 10^{-7}$ H/m, $G_1 = 3 \cdot 10^{-8}$ S/m, $C_1 = 2 \cdot 10^{-10}$ F/m is connected in cascade with an overhead line of length $d_2 = 50$ m and parameters per unit length $R_2 = 7 \cdot 10^{-4} \Omega/\text{m}$, $L_2 = 2 \cdot 10^{-6}$ H/m, $G_2 = 1 \cdot 10^{-9}$ S/m, $C_2 = 10^{-11}$ F/m. A voltage pulse in the form of one half of sinusoidal curve is applied at the beginning of the cable line.

$$0 < t < T_p / 2:$$

$$u_0(t) = u(0, t) = 100 \sin \omega t, \quad f = 10^6 \text{ Hz},$$

$$T_p / 2 = 5 \cdot 10^{-7} \text{ s},$$

$$t > T_p / 2: \quad u_0(t) = u(0, t) = 0.$$

The end of the overhead line is loaded by

1. Resistance $R_e = 100 \Omega$,
2. Serial combination of lumped parameters $R_e = 20 \Omega$ and $L_e = 0.5$ H.

After verification of the convergence on a grid with $\Delta x_1 = \Delta x_2 = 1$ m, $\Delta t = 3 \cdot 10^{-9}$ s ($\Delta t_{k1} = 8.945 \cdot 10^{-9}$ s, $\Delta t_{k2} = 4.472 \cdot 10^{-9}$ s, see (12) and (13)) we calculated for load of type 1) ($R = 100 \Omega$) distribution of the voltage waveforms along both lines (Fig. 5) for various time instants t_p :

- $t_p = 2.25 \cdot 10^{-7}$ s – the wave front reached approximately one half ($d_1 / 2$) of the cable line,
- $t_p = 4.50 \cdot 10^{-7}$ s – the wave front reached approximately the interface (d_1) between the cable and overhead lines,

- $t_p = 5.58 \cdot 10^{-7}$ s – propagation of the reflected wave from the interface causing overvoltage along the cable, while the basic wave passes through the overhead line
- $t_p = 6.30 \cdot 10^{-7}$ s – the basic wave passed through the overhead line and enters the load circuit, which causes propagation of a reflected wave along this line; reflected wave along the cable line approximately reaches its beginning.
- $t_p = 7.00 \cdot 10^{-7}$ s – reflected waves propagate along both lines, which results in higher overvoltage.

The wave process on both lines is in a qualitative accordance with the case of propagation of a rectangular wave presented in references (see [3], page 572). Even in that case overvoltage reaches a value that is almost two times higher than the operation voltage.

Fig. 6 depicts time dependencies of voltages at the beginning of the cable line ($x=0$, curve A), at the place of interface of both lines ($x=50$ m, curve B) and at the end of the cable line ($x=100$ m, curve C) for load $R_e = 100 \Omega$. Fig. 7 shows time dependencies at the same places for load consisting of the serial combination of $R_e = 20 \Omega$ and $L_e = 0.5$ H. In both cases the resultant overvoltage is well observable.

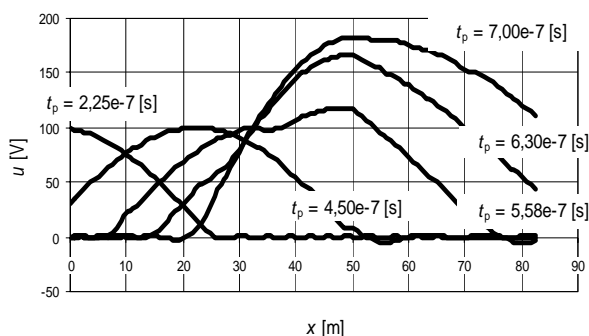


Fig. 5. Illustrative example: distribution of voltage waveforms along both lines at various time instants t_p for load $R_e = 100 \Omega$

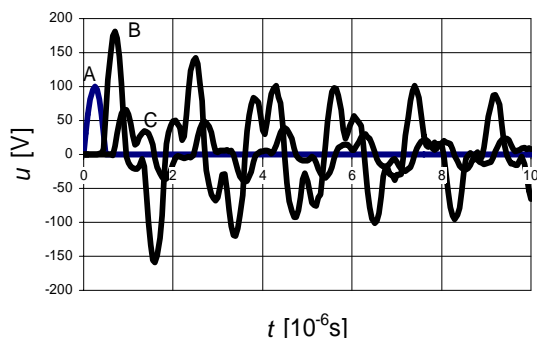


Fig. 6. Illustrative example: time dependencies of voltage at the beginning of the cable line ($x=0$, curve A), at the place of interface of both lines ($x=50$ m, curve B) and at the end of the cable line ($x=100$ m, curve C) for load $R_e = 100 \Omega$

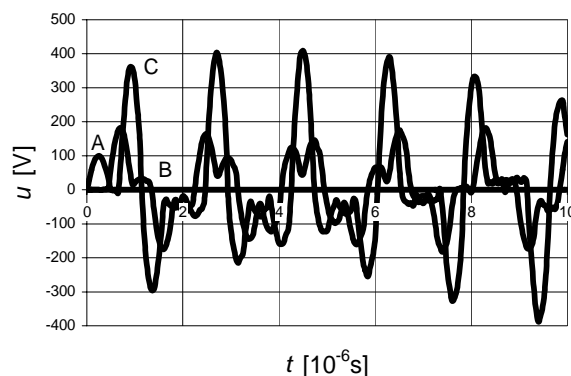


Fig. 7. Illustrative example: time dependencies of voltage at the beginning of the cable line ($x=0$, curve A), at the place of interface of both lines ($x=50$ m, curve B) and at the end of the cable line ($x=100$ m, curve C) for load $R_e = 20 \Omega$ and $L_e = 0.5$ H

VI. CONCLUSION

The paper represents the first part of the project and contains formulation of a computation algorithm for numerical calculation of transients on a one-phase line uniform by parts. In the next work this algorithm will be extended to three-phase lines and then to more complex circuit structures with distributed parameters. Finally it will be used for solution of surge phenomena in electrical power systems including supplied devices (transformers, rotating machines).

REFERENCES

- [1] I. Doležel, V. Valouch, J. Škrmlík, "Wave phenomena in transistor PWM inverter-fed induction motor", Acta Technica CSAV, 41, 1996, No.3, pp. 311–329.
- [2] J. Valsa, "Time-domain simulation of networks containing elements by frequency-domain responses". Journ. of El. Eng., 47, 1996, No. 7–8, pp.170–185.
- [3] D. Mayer, B. Ulrych, "A numerical solution of networks with distributed parameters", Acta Technica CSAV, 42, 1997, pp. 115–127.
- [4] K. Agraval Ashok et al, "Transient response of multiconductor transmission lines excited by a nonuniform electromagnetic field", IEEE Trans. of Electromagnetic Compatibility, EMC-22, No. 2, 1980, pp. 119–129.
- [5] D. Mayer, "Introduction to the network theory", SNTL/ALFA Praha, 2. edition 1981 (in Czech).
- [6] K. W. Morton, D. F. Meyers, "Numerical solution of partial differential equations", Cambridge University Press, Cambridge 1994.